Directed Evolution

DOI: 10.1002/anie.200904209

Creation of an Amino Acid Network of Structurally Coupled Residues in the Directed Evolution of a Thermostable Enzyme**

Manfred T. Reetz, Pankaj Soni, Juan Pablo Acevedo, and Joaquin Sanchis*

The traditional view of enzymes as being composed of dense networks of amino acids that interact locally is widely accepted, yet it is incomplete.[1] Recent research has shown that protein function is also influenced substantially by nonlocal, long-range interactions between residues in a communicating amino acid network.[1,2] It is not a trivial task to identify the precise nature of this phenomenon on a molecular level, but it has in fact been postulated in some enzyme-catalyzed processes,[3] in allosteric regulation of proteins,[1,4] and in information transfer between distal functional surfaces on signaling proteins.[5] Distal effects have been noted in some directed-evolution studies,[6] although their role in putative amino acid networks has not been the focus of interest. Efficiency in laboratory evolution[6,7] may well depend on the occurrence of such interacting residues in an amino acid network, because this would maximize the probability of cooperative effects. Can laboratory evolution create new amino acid networks by forming communicating links between distal residues? Here we show that this is indeed possible, specifically in the thermostabilization of an enzyme.

We recently developed iterative saturation mutagenesis (ISM) as an expedient method for rapid laboratory evolution; the enzyme properties that can be handled successfully are enantioselectivity, substrate scope, and thermostability.[8] Appropriately chosen sites (A, B, C, etc.), each comprising one or more amino acid positions, are subjected to saturation mutagenesis/screening in an iterative manner. In the case of thermostabilization, those residues are chosen which have the highest average B-factor (B-FIT method)[9] corresponding to flexible sites.[10] In a case study[9] involving the lipase from *Bacillus subtilis* (LipA),[11] eight such sites (A–H) were chosen for saturation mutagenesis; all of them (except Tyr139 at site F) are loop residues on the surface of the enzyme, spatially remote from one another. A five-step iterative pathway, E→EG→EGF→EGFD→EGFDB, led to the evolution of a hyperthermophilic mutant XI, characterized by five point mutations Met134Asp (site E), Ile157Met (site G), Tyr139Cys (site F), Lys112Asp (site D), and Arg33Gly (site B), which accumulated stepwise in this order. The T_{50}^{60} value[10] increased from 48 °C to 93 °C, an unprecedented increase in thermostability, which required the screening of only 8000 transformants.[9] Mutant XI shows essentially identical activity and enantioselectivity at room temperature as the wild-type (WT) LipA.

In order to gain insight into the iterative process, which would explain the efficacy of the method, a special deconvolution strategy[12] was applied to mutant XI. We envisioned the experimental construction of a fitness-pathway landscape comprising 5! = 120 pathways leading from WT LipA to mutant XI, without introducing any new amino acid substitutions. This would not only reveal the number of favored pathways (lacking undesired local minima) in a defined segment of protein sequence space, it would also allow us to analyze all epistatic interactions[13] between any two point mutations and between all possible sets of point mutations as defined by additive, partially additive, cooperative, or antagonistic effects. Cooperativity between distal residues would signal the possible existence of structurally coupled residues in an amino acid network. Using conventional site-specific mutagenesis, we first prepared 26 new mutants as outlined in Figure 1. Variants corresponding to E, EG, EGF, and EGFD in addition to the WT and the final variant XI (i.e., EGFDB) were already available as described in the original study.[9]

Since the five point mutations and the thermostability data constitute six parameters, a six-dimensional surface would be required to describe the experimental results, which is difficult to represent graphically. Therefore, the graphics were simplified by stacking the five evolutionary stages of all 120 trajectories linking the WT LipA with mutant XI. The

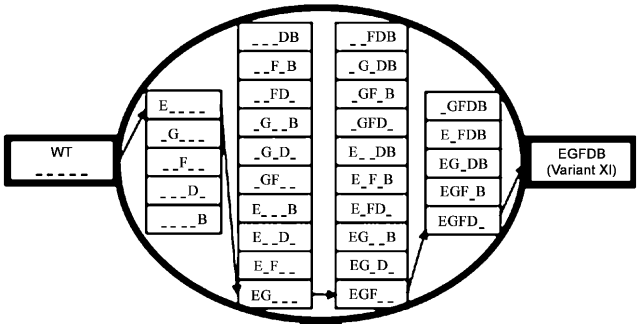

Figure 1. The 30 possible mutants as intermediate stages between the WT LipA and enzyme variant XI (corresponding to EGFDB) based on the use of the five point mutations. The connecting lines indicate the original trajectory E→EG→EGF→EGFD→EGFDB, which is one of the 120 possible pathways.

[*] Prof. Dr. M. T. Reetz, Dr. P. Soni, Dr. J. P. Acevedo, Dr. J. Sanchis
Max-Planck-Institut für Kohlenforschung
Kaiser-Wilhelm-Platz 1, 45470 Mülheim an der Ruhr (Germany)
Fax: (+49) 208-306-2985
E-mail: reetz@mpi-muelheim.mpg.de
Homepage: http://www.mpi-muelheim.mpg.de/mpikofo_home.html

[**] We thank J. D. Carballeira for helpful discussions. This work was supported by the Fonds der Chemischen Industrie and the Deutsche Forschungsgemeinschaft (SSP 1170 "Directed Evolution").

Supporting information for this article is available on the WWW under http://dx.doi.org/10.1002/anie.200904209.

result of this procedure is shown in Figure 2, which reveals two types of trajectories, favored pathways (green) lacking local minima and disfavored pathways (red) characterized by the occurrence of at least one local minimum. Detailed

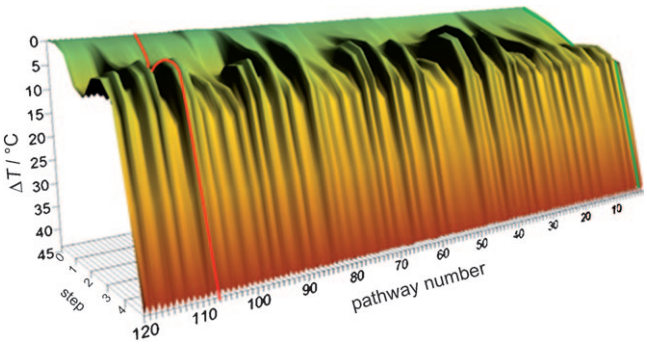

Figure 2. Fitness-pathway landscape featuring the 120 trajectories leading from the WT Lip A to the thermostabilized mutant XI. A typical favored pathway is featured in green (number 1), a typical disfavored pathway in red (number 107).

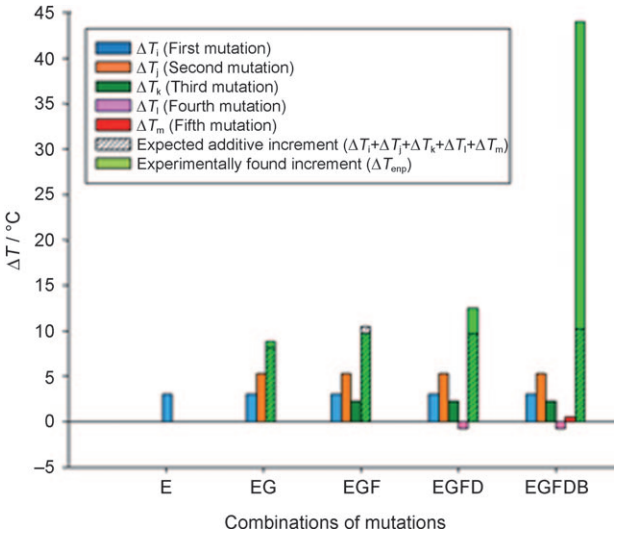

Figure 3. Epistatic interactions among the point mutations according to Equation (1) at every stage along the original favored pathway E→EG→EGF→EGFD→EGFDB (trajectory 1).

analysis including data of all trajectories (see Figure S1 in the Supporting Information) points to the presence of 40 favored pathways, which is a notably high number considering the fact that no additional amino acid substitutions are allowed in the deconvolution process. The other 80 trajectories linking WT LipA with mutant XI contain local minima; backtracking puts the evolutionary process back on a positive track.

In order to analyze quantitatively all epistatic interactions[13] between two point mutations (*i* and *j*) at every stage of a given trajectory in terms of additive, less than additive, antagonistic, or cooperative (synergistic) effects, we utilized Equation (1),

$$\Delta T_{ij} = \Delta T_{exp} - (\Delta T_i + \Delta T_j) \quad (1)$$

where ΔT_{exp} is the experimentally observed difference in $T_{50}{}^{15}$ values, and ΔT_i and ΔT_j refer to the experimentally observed changes in $T_{50}{}^{15}$ values caused by each mutant separately. Thus, the values of ΔT_{ij} indicate either cooperative effects ($\Delta T_{ij} > 0$), additive effects meaning no interaction ($\Delta T_{ij} = 0$), partially additive effects ($\Delta T_{ij} < 0$) and [(ΔT_i and ΔT_j) < ΔT_{exp}], or they signal antagonistic effects ($\Delta T_{ij} < 0$) and [(ΔT_i or ΔT_j) > ΔT_{exp}].

We first focus on the analysis of the original pathway E→EG→EGF→EGFD→EGFDB (trajectory 1). Figure 3 shows that the interactions among the point mutations are essentially additive at the first two steps of the evolutionary process (EG and EGF), and that cooperativity prevails thereafter, reaching a dramatic stage at EGFDB. The structural change at site B is characterized by the point mutation Arg33Gly, which when introduced alone in the WT causes only a minute improvement in thermostability. Moreover, the point mutations introduced at the other sites, E, G, and F, likewise induce only small improvements in thermostability, and the single point mutation at site D actually has an antagonistic influence. In combination with the first four point mutations, however, the introduction of glycine at position 33 orchestrates pronounced cooperativity in what can be called a "zip effect" suggesting the creation of a structurally coupled amino acid network. Here and in all other pathways the mutations in the initial steps lead to small increases in thermostability relative to the final improvement, reminiscent of a neutral drift.[14] Clearly, none of the point mutations are superfluous; this also pertains to the other 39 favored pathways, indicating high efficiency of the B-FIT approach. It should be pointed out that in some previous protein-engineering studies regarding thermostabilization, additive and nonadditive effects,[13] especially in double-mutant cycles, have been postulated on the basis of partial deconvolution,[6,10,11b,15] but deep-seated analyses of the type exemplified in Figure 3 were not performed.

Using the experimental results (see Tables S2 and S3 in the Supporting Information), it is possible to analyze all 120 pathways in a similar manner. In seven other favored trajectories the last step likewise involves the mutation Arg33Gly, which again results in a sudden increase in thermostability (see Table S4 in the Supporting Information). The introduction of glycine may come as a surprise because this amino acid is generally considered to increase flexibility. However, the B-FIT approach is simply a guide for choosing appropriate sites for amino acid randomization. It does not mean that the B-factor at such a site will necessarily decrease, nor does it mean that this is the only place in the enzyme at which rigidity/flexibility may change as a result of a point mutation. It is tempting to speculate that the flexibility of glycine actually makes the zip effect possible. However, in the final step of the 40 favored trajectories, seven involve site F (Tyr139Cys), fifteen involve site D (Lys112Asp), and ten involve site G (Ile157Met), whereas the mutation at site E (Met134Asp) never occurs at the terminus of the five-step process in a favored pathway (see Table S4 in the Supporting Information). Epistatic interactions in all permutationally possible double, triple, and quadruple mutants were also analyzed (see Figures S2–S4 in the Supporting Information).

None of them constitute mutants that have a higher thermostability than variant XI, and all of them show notable cooperative effects.

The analysis of disfavored pathways is also informative; pathway 107 serves as a typical example (see Figure S5 in the Supporting Information). In these cases, local minima occur, caused most often by antagonistic effects operating between certain point mutations or sets of point mutations. Further combinations along the evolutionary pathway completely purge any negative epistatic effects by inducing strong cooperativity between distal residues. In other cases of a local minimum, the cooperative effect at one stage is higher than in the step that follows. Escaping from a local minimum is possible by backtracking, i.e., by going back one or two stages, which puts the evolutionary process back on a favored trajectory.

Unveiling the reason(s) for the pronounced cooperative effects on a molecular level would throw light on the nature of the postulated amino acid network, but this is a challenging task that requires further experimentation including X-ray structural and NMR analyses of LipA and mutant XI. At this point we report the results of molecular dynamics (MD) calculations of three forms of the enzyme, namely the WT LipA, the second-to-last mutant EGFD, and the final mutant XI (EGFDB) occurring in the original pathway (E→EG→EGF→EGFD→EGFDB). The simulations provide some insightful information. We used the OPLS-AA/TIP3P force field with the Desmond program.[16] All simulations were run during 2 ns with a recording interval of 1.2 ps (see the Supporting Information for more details and analyses). After simulation equilibration, different conformers (in ensembles) were selected along the trajectories, then hydrogen-bonding correlation plots derived from each of them were constructed.[17] These plots are useful tools for analyzing tertiary hydrogen-bond networks and for illuminating the principal differences amongst the WT LipA and the mutants (see Figure S6 in the Supporting Information).

The results point to an intriguing phenomenon, namely that mutant XI is characterized by a new hydrogen-bond network on the surface in the form of a continuous surface band, connecting most of the flexible loops present in the WT LipA. Surprisingly, only one of the five point mutations participate directly in this network, while essentially all surface H bonds in the WT are retained in the best mutant XI (for clarity this is not shown in the Figures).

Figure 4 shows the whole backbone structure of the WT LipA and the second-to-last mutant EGFD, featuring several small and isolated H-bond regions, which in the final mutant XI become part of the extensive and fully linked amino acid network characterized by H bonds and salt bridges (Figure 4). This means that the last point mutation at site B (Arg33Gly) in the original pathway induces extensive structural coupling of distal residues, which we interpret as the origin of the zip effect.

In the analysis that follows (see also Figure S7 in the Supporting Information for a schematic topology diagram), we consider for easy reading Asp118 as the beginning of the connecting band and proceed stepwise to the other end. It becomes clear that the new H bonds in mutant XI connect in the first segment of the network the loops harboring Leu102–Ile123 and Gly67–Val71, the N terminus, and the loop containing Val27–Lys35. This segment includes the following H bonds: Asp118/Lys70, Lys70/Asn4, and His3/Ser32 (see

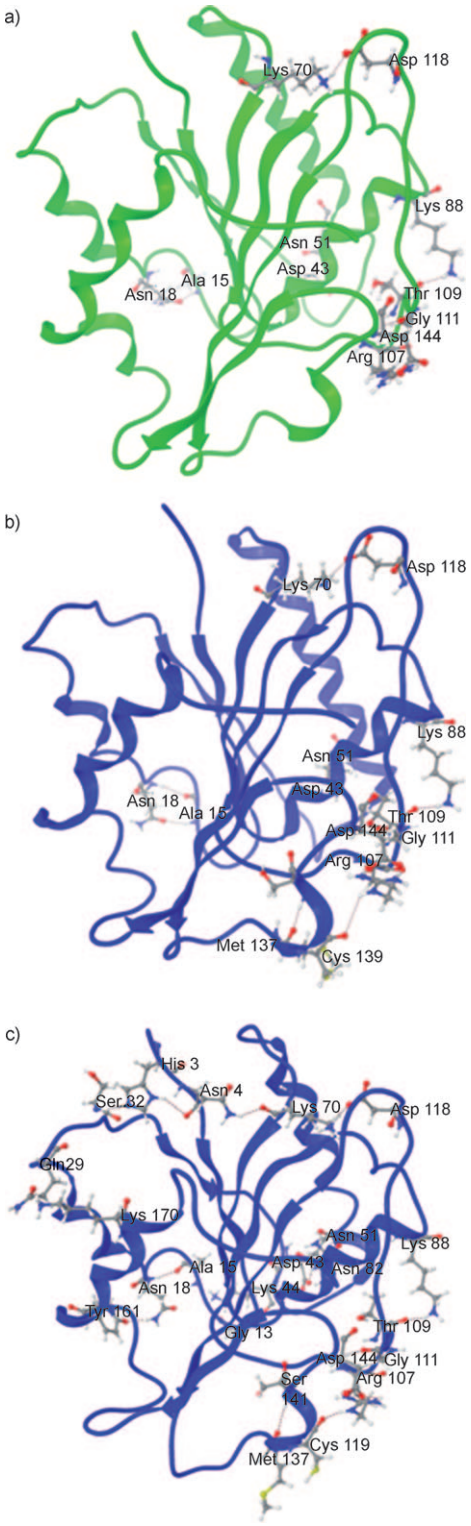

Figure 4. Crucial hydrogen bonds and salt bridges in a) WT LipA, b) second-to-last mutant EGFD, and c) mutant XI (EGFDB), which features an extended network of hydrogen bonds and salt bridges in structurally coupled residues (see text).

Figure S8d in the Supporting Information). According to the MD equilibration, WT LipA and mutant EGFD have only the Asp118/Lys70 interaction, but not the Lys70/Asn4 or His3/Ser32 interactions (see Figure S8a and Table S5 in the Supporting Information). This introduces a higher degree of rigidity of the respective structural segments, leading to enhanced thermostability. This conclusion is corroborated by the RMSD (root mean square deviation) values calculated for the loops and the N terminus. Going forward along the H-bond network, loop Val27–Lys35 and the αF helix (see Figure S8d in the Supporting Information) are linked through the H bonding of Gln29/Lys170, again a connection that is absent in WT LipA and with a very low frequency in the second-to-last mutant EGFD. The subsequent H bonds go through the α helix leading up to Tyr161. The H bond Tyr161/Asn18 connects this rigid α helix with the loop His10–Phe19 (see Figure S8e in the Supporting Information). WT LipA does not show any H-bond connection in this segment, and such connections in mutant EGFD appear in only a few conformers. Going "forward" in the band, loop His10–Phe19, loop Asp40–Asn51 and the αC helix are linked through a continuous H-bond system which includes Asn18, Ala15, Gly13, Lys44, Asp43, and Asn82 (see Figure S8e in the Supporting Information). Finally, the H bond Lys88/Thr109 connects the αC helix with the loop Leu102–Ile123, which themselves follow additional H bonds linking this last loop with loop Ser132–Ala146 (see Figure S8f in the Supporting Information). The latter comes about through the H bond of Arg107/Cys139, and simultaneously through Arg107 and Gly111, which form H bonds with the side-chain and backbone nitrogen of Asp144, respectively. Another H bond participating in the surface network of this segment is Met137/Ser141. Structurally, the previously described segment in mutant XI appears to be almost the same as that in the mutant EGFD. It differs from that of WT LipA in which the H bonds Arg107/Cys139 (in WT LipA corresponding to Arg107/Tyr139) and Met137/Ser141 are absent.

Only the point mutation at site F (Tyr139Cys) participates directly in the newly created H-bond network. This surprising result serves as a warning in the interpretion of results of directed evolution studies because focusing solely on the actual point mutations may blend out important structural manifestations occurring elsewhere. In addition to the previous effects, the MD calculations suggest that every mutation induces slight side-chain conformational changes in the vicinity, which assist the ultimate networking in the last step of the evolutionary process. Mutation Arg33Gly (site B) is involved in connecting loop Gly67–Val71, the N terminus, loop Val27–Lys35, and the αF helix. Mutations at sites D, F, and E contribute cooperatively to make a more intricate H-bond connections in last segment of the H-bond network, including new H bonds such as Arg107/Cys139 and Met137/Ser141, which stabilize and connect the αC helix, loop Leu102–Ile123, and loop Ser132–Ala146. Mutation at site G seems to induce the formation of the H bond Asn18/Tyr161 through hydrophobic interaction with Leu160; this affects positioning of Tyr161 or restricts directly the motion of Asn18. This H bond connects the αF helix and the loop His10–Phe19. For additional comments see the Supporting Information; for details regarding the distance between donor and acceptor atoms of H bonds in the network see Figure S9 in the Supporting Information).

Finally, we have performed packing density calculations[18] which predict, inter alia, higher packing densities at the C- and N-terminal segments of mutant XI relative to those of mutant EGFD (see Packing Density Calculations in the Supporting Information). It is likely that this phenomenon likewise contributes to the enormously high thermostability of this mutant enzyme.

This discussion does not cover all features of the amino acid network, nor do we address all effects that may possibly be operating on a molecular level.[10,11b] For example, in a study regarding the thermostabilization of LipA based on epPCR, which led to very different point mutations, Sankaranarayanan, Rao, and co-workers postulated stacking of tyrosines, peptide plane flipping and other subtle effects.[11b] Suffice it to say that the zip effect in our study includes cooperative interactions in long-range as well as local communication. Other factors yet to be studied may also play a role; for example, the structural changes brought about on the surface by the long-range cooperative effects may well influence the way the enzyme interacts with the environment (water, protein–protein interactions, etc.).

In conclusion, we have applied a systematic deconvolution strategy which allows the analysis of epistatic effects operating between the evolved five point mutations and between all combinations thereof at all stages of a five-step evolutionary process based on the B-FIT method,[9] in which the thermostability of the lipase from *Bacillus subtilis* (LipA) was increased by 45 °C. We also constructed the fitness-pathway landscape featuring 120 pathways leading from the WT LipA to the thermostabilized mutant XI, and likewise analyzed the respective epistatic interactions. The crucial lesson learned from the detailed analyses is the realization of pronounced cooperative effects between distal residues, especially in the final step of the evolutionary process. MD simulations point to the stepwise formation of an extensive H-bond/salt-bridge network of structurally coupled residues on the surface of the enzyme. All five point mutations are necessary for high thermostability, yet only one of them participates directly in the extended network. At this point it is not certain whether the zip effect will always accompany B-FIT studies, although cooperative effects can be expected. In future protein engineering research, the laboratory evolution and identification of structural and functional amino acid networks as described herein deserves increased attention.

Received: July 29, 2009
Published online: September 28, 2009

Keywords: directed evolution · enzymes · hydrogen bonds · protein modifications · saturation mutagenesis

[1] J. Lee, M. Natarajan, V. C. Nashine, M. Socolich, T. Vo, W. P. Russ, S. J. Benkovic, R. Ranganathan, *Science* **2008**, *322*, 438–442.

[2] a) M. Vendruscolo, N. V. Dokholyan, E. Paci, M. Karplus, *Phys. Rev. E* **2002**, *65*, 061910; b) C. Lücke, S. Huang, M. Rademacher,

H. Rüterjans, *Protein Sci.* **2202**, *11*, 2382 – 2392; c) L. H. Greene, V. A. Higman, *J. Mol. Biol.* **2003**, *334*, 781 – 791; d) X. Jiao, S. Chang, C. Li, W. Chen, C. Wang, *Phys. Rev. E* **2007**, *75*, 051903; e) C. Böde, I. A. Kovács, M. S. Szalay, R. Palotai, T. Korcsmáros, P. Csermely, *FEBS Lett.* **2007**, *581*, 2776 – 2782; f) S. Chang, X. Jiao, X. Gong, C. Li, W. Chen, C. Wang, *Phys. Rev. E* **2008**, *77*, 061920; g) B.-C. Lee, K. Park, D. Kim, *Proteins Struct. Funct. Bioinf.* **2008**, *72*, 863 – 872; h) T. Yu, X. Zou, S.-Y. Huang, X.-W. Zou, *J. Theor. Biol.* **2009**, *256*, 408 – 413.

[3] a) S. Hammes-Schiffer, S. J. Benkovic, *Annu. Rev. Biochem.* **2006**, *75*, 519 – 541; b) K. Henzler-Wildman, D. Kern, *Nature* **2007**, *450*, 964 – 972; c) I. Bahar, C. Chennubhotla, D. Tobi, *Curr. Opin. Struct. Biol.* **2007**, *17*, 633 – 640; d) N. Tokuriki, D. S. Tawfik, *Science* **2009**, *324*, 203 – 207.

[4] a) A. del Sol, H. Fujihashi, D. Amoros, R. Nussinov, *Mol. Syst. Biol.* **2006**, 1 – 12; b) M. Resch, H. Striegl, E. M. Henssler, M. Sevvana, C. Egerer-Sieber, E. Schiltz, W. Hillen, Y. A. Muller, *Nucleic Acids Res.* **2008**, *36*, 4390 – 4401; c) A. Whitty, *Nat. Chem. Biol.* **2008**, *4*, 435 – 439; d) N. M. Goodey, S. J. Benkovic, *Nat. Chem. Biol.* **2008**, *4*, 474 – 482; e) M. D. Daily, J. J. Gray, *PLoS Comput. Biol.* **2009**, *5*, e1000293.

[5] J. F. Swain, L. M. Gierasch, *Curr. Opin. Struct. Biol.* **2006**, *16*, 102 – 108.

[6] Reviews of directed evolution: a) S. Lutz, U. T. Bornscheuer, *Protein Engineering Handbook*, *Vol. 1–2*, Wiley-VCH, Weinheim, **2009**; b) K. M. Arndt, K. M. Müller, *Protein Engineering Protocols (Methods in Molecular Biology)*, *Vol. 352*, Humana Press, Totowa, NJ, **2007**; c) F. H. Arnold, G. Georgiou, *Methods and Molecular Biology*, *Vol. 230*, Humana, Totowa, NJ, **2003**; d) C. Jäckel, P. Kast, D. Hilvert, *Annu. Rev. Biophys. Biomol. Struct.* **2008**, *37*, 153 – 173; e) S. Brakmann, A. Schwienhorst, *Evolutionary Methods in Biotechnology—Clever Tricks for Directed Evolution*, Wiley-VCH, Weinheim, **2004**; f) E. G. Hibbert, F. Baganz, H. C. Hailes, J. M. Ward, G. J. Lye, J. M. Woodley, P. A. Dalby, *Biomol. Eng.* **2005**, *22*, 11 – 19; g) S. B. Rubin-Pitel, H. Zhao, *Comb. Chem. High Throughput Screening* **2006**, *9*, 247 – 257; h) J. Kaur, R. Sharma, *Crit. Rev. Biotechnol.* **2006**, *26*, 165 – 199; i) S. Bershtein, D. S. Tawfik, *Curr. Opin. Chem. Biol.* **2008**, *12*, 151 – 158; j) M. T. Reetz in *Asymmetric Organic Synthesis with Enzymes* (Eds.: V. Gotor, I. Alfonso, E. García-Urdiales), Wiley-VCH, Weinheim, **2008**, pp. 21 – 63.

[7] a) S. Lutz, W. M. Patrick, *Curr. Opin. Biotechnol.* **2004**, *15*, 291 – 297; b) R. J. Fox, G. W. Huisman, *Trends Biotechnol.* **2008**, *26*, 132 – 138; c) T. S. Wong, D. Roccatano, M. Zacharias, U. Schwaneberg, *J. Mol. Biol.* **2006**, *355*, 858 – 871; d) J. D. Bloom, M. M. Meyer, P. Meinhold, C. R. Otey, D. MacMillan, F. H. Arnold, *Curr. Opin. Struct. Biol.* **2005**, *15*, 447 – 452.

[8] M. T. Reetz, D. Kahakeaw, J. Sanchis, *Mol. BioSyst.* **2009**, *5*, 115 – 122.

[9] a) M. T. Reetz, J. D. Carballeira, A. Vogel, *Angew. Chem.* **2006**, *118*, 7909 – 7915; *Angew. Chem. Int. Ed.* **2006**, *45*, 7745 – 7751; b) M. T. Reetz, J. D. Carballeira, *Nat. Protoc.* **2007**, *2*, 891 – 903.

[10] Recent reviews of enzyme thermostabilization by protein engineering: a) V. G. H. Eijsink, S. Gåseidnes, T. V. Borchert, B. van den Burg, *Biomol. Eng.* **2005**, *22*, 21 – 30; b) C. Ó'Fágáin, *Enzyme Microb. Technol.* **2003**, *33*, 137 – 149; c) A. S. Bommarius, J. M. Broering, *Biocatal. Biotransform.* **2005**, *23*, 125 – 139; d) S. Radestock, H. Gohlke, *Eng. Life Sci.* **2008**, *8*, 507 – 522.

[11] a) X-ray structure of LipA used in the study:[9] K. Kawasaki, H. Kondo, M. Suzuki, S. Ohgiya, S. Tsuda, *Acta Crystallogr. Sect. D* **2002**, *58*, 1168 – 1174; b) Thermostabilization of LipA by directed evolution using epPCR: P. Acharya, E. Rajakumara, R. Sankaranarayanan, N. M. Rao, *J. Mol. Biol.* **2004**, *341*, 1271 – 1281.

[12] M. T. Reetz, J. Sanchis, *ChemBioChem* **2008**, *9*, 2260 – 2267.

[13] a) D. C. Carter, G. Winter, A. J. Wilkinson, A. R. Fersht, *Cell* **1984**, *38*, 835 – 840; b) J. A. Wells, *Biochemistry* **1990**, *29*, 8509 – 8517; c) A. Horovitz, *Curr. Biol.* **1996**, *6*, R121 – R126; d) A. S. Mildvan, *Biochemistry* **2004**, *43*, 14517 – 14520; e) C. M. Yuen, D. R. Liu, *Nat. Methods* **2007**, *4*, 995 – 997.

[14] S. Bershtein, K. Goldin, D. S. Tawfik, *J. Mol. Biol.* **2008**, *379*, 1029 – 1044.

[15] a) A. Y. Istomin, M. M. Gromiha, O. K. Vorov, D. J. Jacobs, D. R. Livesay, *Proteins Struct. Funct. Genet.* **2008**, *70*, 915 – 924; b) J. F. Chaparro-Riggers, K. M. Polizzi, A. S. Bommarius, *Biotechnol. J.* **2007**, *2*, 180 – 191; c) K. Numata, M. Muro, N. Akutsu, Y. Nosoh, A. Yamagishi, T. Oshima, *Protein Eng.* **1995**, *8*, 39 – 43.

[16] a) K. J. Bowers, E. Chow, H. Xu, R. O. Dror, M. P. Eastwood, B. A. Gregersen, J. L. Klepeis, I. Kolossváry, M. A. Moraes, F. D. Sacerdoti, J. K. Salmon, Y. Shan, D. E. Shaw, *Proceedings of the ACM/IEEE Conference on Supercomputing (SC06)*, Tampa, Florida, November 11 – 17, **2006**; b) D. S. Cerutti, R. Duke, P. L. Freddolino, H. Fan, T. P. Lybrand, *J. Chem. Theory Comput.* **2008**, *4*, 1669 – 1680; c) I. T. Arkin, H. Xu, M. Ø. Jensen, E. Arbely, E. R. Bennett, K. J. Bowers, E. Chow, R. O. Dror, M. P. Eastwood, R. Flitman-Tene, B. A. Gregersen, J. L. Klepeis, I. Kolossváry, Y. Shan, D. E. Shaw, *Science* **2007**, *317*, 799 – 803.

[17] a) I. K. McDonald, J. M. Thornton, *J. Mol. Biol.* **1994**, *238*, 777 – 793; b) Z. Bikadi, L. Demko, E. Hazai, *Arch. Biochem. Biophys.* **2007**, *461*, 225 – 234.

[18] a) A. Goede, R. Preissner, C. Frömmel, *J. Comput. Chem.* **1997**, *18*, 1113 – 1123; b) K. Rother, P. W. Hildebrand, A. Goede, B. Gruening, R. Preissner, *Nucl. Acids. Res.* **2009**, D393 – D395.

